Bacterial in-cell NMR of human α-synuclein: a disordered monomer by nature?

Andres Binolfi, Francois-Xavier Theillet and Philipp Selenko[1]

In-cell NMR Group, Department of NMR-Assisted Structural Biology, Leibniz Institute of Molecular Pharmacology (FMP Berlin), Robert-Roessle-Strasse 10, Berlin 13125, Germany

Abstract

The notion that human α-synuclein is an intrinsically disordered monomeric protein was recently challenged by a postulated α-helical tetramer as the physiologically relevant protein structure. The fact that this alleged conformation had evaded detection for so many years was primarily attributed to a widely used denaturation protocol to purify recombinant α-synuclein. In the present paper, we provide in-cell NMR evidence obtained directly in intact *Escherichia coli* cells that challenges a tetrameric conformation under native *in vivo* conditions. Although our data cannot rule out the existence of other intracellular protein states, especially in cells of higher organisms, they indicate clearly that inside *E. coli* α-synuclein is mostly monomeric and disordered.

Structural features of human α-synuclein

α-Synuclein is expressed abundantly in brain dopaminergic neurons and its aggregation into amyloid fibrils has been correlated strongly with the onset of PD (Parkinson's disease) and neurodegeneration [1,2]. α-Synuclein contains 140 amino acids and can be divided into three main regions according to its primary sequence. The N-terminal region (residues 1–60) is known to interact with lipid vesicles [3,4], the hydrophobic NAC (non-amyloid-β component) region (residues 61–95) is responsible for protein aggregation [5] and the negatively charged C-terminus (residues 96–140) is reported to counteract α-synuclein aggregation [6–8]. The structural properties of α-synuclein in its soluble form have been investigated extensively. From an early purification study under native conditions by Lansbury and co-workers in 1996, for which SEC (size-exclusion chromatography), native PAGE, sucrose gradient centrifugation and MALDI–TOF (matrix-assisted laser-desorption ionization–time-of-flight)-MS were used, α-synuclein was described as a disordered monomer with an apparent molecular mass of 14.5 kDa [9]. Spectroscopic characterization by CD and FTIR (Fourier-transform IR) spectroscopy did not detect regions of stable secondary structure or a hydrophobic protein core. In the following years, these findings were corroborated by several other groups [10–19]. NMR was later employed to characterize the monomeric solution state of α-synuclein at atomic resolution. ^{13}C chemical shift data demonstrated that the first ~100 residues had propensities to populate transient α-helical structures [20,21]. The C-terminal region of α-synuclein was determined to be less well defined, although short stretches of β-turn-like conformations were identified [17,20]. As expected for a monomeric disordered protein, ^{15}N relaxation data revealed increased backbone amide dynamics compared with those of folded globular proteins [20]. NMR spectroscopy, SAXS (small-angle X-ray scattering), DLS (dynamic light scattering) and fluorescence spectroscopy delineated a solution conformation that was not fully compatible with an extended random-coil state [6,13,22–24]. In turn, transient intramolecular long-range contacts between the N- and C-terminus, as well as the NAC region and C-terminus, of α-synuclein were identified and shown to prevent the central NAC region from spontaneous aggregation into oligomeric fibrils [6,22]. Together, these data established that α-synuclein existed in defined structural ensembles of interconverting monomers, similar to what has also been observed for many other IDPs (intrinsically disordered proteins) [25,26].

Monomeric compared with tetrameric α-synuclein

The disordered monomeric conformation of α-synuclein was challenged recently by two papers that proposed a different structure under physiological conditions [27,28]. These proposed a tetrameric state of the protein with well-defined α-helical segments. Moreover, it was suggested that this α-synuclein conformation had remained undetected to date mainly because of a denaturation protocol that is employed by many groups to purify recombinant α-synuclein. It was stated that the use of denaturing agents or boiling of the bacterial cell lysates during the initial purification steps of recombinant α-synuclein could destroy the tetramer and result in the accumulation of the disordered monomer [27,28]. Endogenous α-synuclein isolated from RBCs (red blood cells), different cultured neuronal cell lines and human tissue under non-denaturing conditions was reported to occur predominantly as a native tetramer of approximately 58 kDa,

Key words: amyloid, in-cell nuclear magnetic resonance (in-cell NMR), intrinsically disordered protein (IDP), α-synuclein, tetramer.

Abbreviations used: BOG, octyl β-D-glucopyranoside; HSQC, heteronuclear single-quantum coherence; NAC, non-amyloid-β component; SEC, size-exclusion chromatography.

[1]To whom correspondence should be addressed (email selenko@fmp-berlin.de).

on the basis of analytical ultracentrifugation, native PAGE, transmission scanning electron microscopy and *in vitro* cross-linking of the protein [27]. A similar hypothetical α-synuclein tetramer was also purified from *Escherichia coli*, although in this case the α-synuclein construct contained ten additional amino acids at its N-terminus [28]. CD spectra of α-synuclein purified under non-denaturing conditions suggested a high α-helical content in both studies. Monomeric α-synuclein was shown to bind to lipid vesicles, leading to the formation of stable α-helical segments within its first 100 residues [29,30]. The alleged α-synuclein tetramer was reported to bind membranes with higher affinity than the disordered monomer [27]. Finally, the proposed native tetrameric form of α-synuclein displayed a reduced tendency to form amyloid fibrils and was non-toxic when added to cultured neuronal cells [27,28]. According to $^{13}C\alpha$ and $^{1}H\alpha$ NMR chemical shift data, the N-terminally extended tetrameric form of α-synuclein exhibited 'significant' helical propensities at different N-terminal positions and within the central NAC region [28]. ^{15}N-edited NOESY–HSQC (heteronuclear single-quantum coherence) experiments and CD spectroscopy measurements were reported to confirm these findings. It was noted that two-dimensional ^{1}H-^{15}N correlation NMR spectra of tetrameric α-synuclein failed to detect the characteristic features of α-helical secondary structure, in contrast with what has been observed for monomeric α-synuclein bound to micelles [29,30]. This behaviour was attributed to the dynamic transient nature of the helical regions in the tetramer [28].

Conspicuously, the overall appearance of the two-dimensional NMR spectra of the α-synuclein tetramer closely resembles previous *in vitro* NMR spectra of the monomeric protein [6,7,31,32]. We have used the NMR chemical shift data of the α-synuclein tetramer that have been deposited in the Biological Magnetic Resonance Data Bank (BRMB #17665) [28] to emulate a two-dimensional ^{1}H-^{15}N correlation spectrum of this protein state. We then compared this virtual NMR spectrum with a two-dimensional ^{1}H-^{15}N correlation spectrum that we recorded *in vitro* on a sample of recombinant monomeric α-synuclein, purified under denaturing conditions, but resuspended in the same buffer used for collecting the deposited tetramer chemical shifts. A superposition of these NMR spectra (Figure 1A) shows that they are very similar. Differences were only seen for the deposited chemical shifts of Tyr^{39} and Leu^{113}. Line broadening of Ser^{42}, Asn^{103} and of residues in the glycine region of the NMR spectrum was due to known unfavourable chemical exchange effects at this temperature and pH (i.e. 25°C and pH 7.4). These observations are in line with previously published data [21]. For two-dimensional ^{1}H-^{15}N NMR spectra recorded on the same sample at 10°C, previously line-broadened resonances were clearly visible (results not shown). These data suggest that the reported differences in chemical shift values between the alleged α-synuclein tetramer and the monomeric form of the protein primarily arise from different solution conditions.

Possible oligomeric states of α-synuclein have been discussed previously. Even the seminal paper by Lansbury and co-workers, in which the first biophysical characterization of α-synuclein was reported, raised the question of whether α-synuclein might exist as an oligomer [9]. The reasons for this were based on concerns about the unusual migration behaviour of α-synuclein on SEC columns and native PAGE (apparent molecular mass ~58 kDa, measured relative to globular protein standards). These observations were interpreted as the monomeric form of α-synuclein having a more elongated shape than the globular protein standards. Further support for this notion was provided by sucrose gradient ultracentrifugation analyses and native PAGE experiments at different acrylamide concentrations, with which molecular masses of ~20 kDa were determined [9]. Higher apparent molecular masses (~57 kDa) have also been obtained for β-synuclein, another synuclein isoform with high sequence homology within the N-terminal protein region, and for other IDPs [33–35]. In 2012, six research groups teamed up to carefully reinvestigate the monomer/tetramer controversy [36]. Employing different native and denaturing purification methods in parallel, α-synuclein from mammalian central nervous system and red blood cells, as well as from *E. coli*, was prepared. The consortium reported that α-synuclein from both types of preparations had similar chromatographic elution profiles and electrophoretic mobility properties, according to molecular mass standards of folded and unfolded proteins. Moreover, the two-dimensional ^{1}H-^{15}N NMR features of α-synuclein purified under non-denaturing conditions closely matched those of protein preparations that were obtained from denaturing purification procedures [36], which collectively argued against the natively folded tetramer conformation. These observations are in agreement with a recent study that stipulated the requirements for N-terminal α-synuclein acetylation and a non-denaturing purification protocol in the presence of glycerol and the non-ionic detergent BOG (octyl β-D-glucopyranoside) in order to recover an oligomeric more α-helical form of α-synuclein from *E. coli* [37]. Because α-synuclein is not naturally acetylated in bacteria, a fission yeast N-terminal acetylation B complex had to be co-expressed for efficient modification. These results also contradict the hypothesis of a folded α-synuclein tetramer in non-acetylation-competent *E. coli* cells.

Insights from in-cell NMR

Because possible differences in α-synuclein conformations caused by denaturing or non-denaturing purification protocols are at the centre of the monomer/tetramer controversy, direct in-cell NMR measurements of α-synuclein in intact *E. coli* cells are well poised to provide insights into the 'native' protein state(s) inside live bacteria. Prokaryotic in-cell NMR experiments do not require any form of sample purification or cell lysis and are therefore ideally suited to investigate the high-resolution structural propensities of α-synuclein in an undisturbed cellular environment [38–42]. In-cell NMR measurements involve NMR isotope labelling (^{15}N and/or ^{13}C) during the induction period of recombinant protein expression and direct NMR readouts on the intact cell

Figure 1 | ***In vitro*** **and in-cell NMR properties of** α**-synuclein**

(**A**) Overlay of two-dimensional ^{1}H-^{15}N SOFAST-HMQC (band-selective optimized flip-angle short-transient heteronuclear multiple quantum coherence) NMR spectra of 150 μM α-synuclein (black), purified under denaturing conditions and dissolved in TNBG buffer (100 mM Tris/HCl, pH 7.4, 100 mM NaCl, 10% glycerol and 0.1% BOG), under the same buffer conditions and temperature settings, i.e. 25°C, as for the tetramer and a virtual ^{1}H-^{15}N HSQC NMR spectrum of the α-synuclein tetramer (red marks) based on deposited BMRB (Biological Magnetic Resonance Bank) chemical shifts. (**B**) Overlay of two-dimensional ^{1}H-^{15}N SOFAST-HMQC (left-hand panel) and two-dimensional (H-flip)^{13}CO-^{15}N (right-hand panel) NMR spectra of monomeric α-synuclein *in vitro* (black) and inside *E. coli* cells (red). Two-dimensional ^{1}H-^{15}N correlations were acquired at 10°C to minimize chemical exchange effects. Two-dimensional ^{13}CO-^{15}N correlations were obtained at 30°C. Labelled α-synuclein residues denote broadened signals in the different panels. Asterisks in (**B**) indicate *E. coli* background signals (see also Supplementary Figure S1A at http://www.biochemsoctrans.org/bst/040/bst0400950add.htm). For simplicity, only the ^{13}CO component corresponding to residue *i* is labelled in the ^{13}CO-^{15}N panel. (**C**) Left-hand panel: Coomassie Blue-stained SDS/PAGE and anti-α-synuclein Western blot. Lanes 1 and 2, total *E. coli* cell lysate before and after induction of recombinant α-synuclein expression respectively; lanes 3–6, loaded reference α-synuclein concentrations, i.e. 3.5, 7, 14 and 28 μM respectively. Molecular masses are indicated in kDa. Right-hand panel: determination of α-synuclein concentrations inside *E. coli* by quantitative Western blotting (WB) and NMR signal integration (NMR). Results are means ± S.D. from two independent experiments. (**D**) ^{13}CO chemical shift differences of α-synuclein resonances *in vitro* and in-cell. Residues broadened beyond detection were not included in the analysis. Experimental details can be found in the Supplementary Online Data at http://www.biochemsoctrans.org/bst/040/bst0400950add.htm.

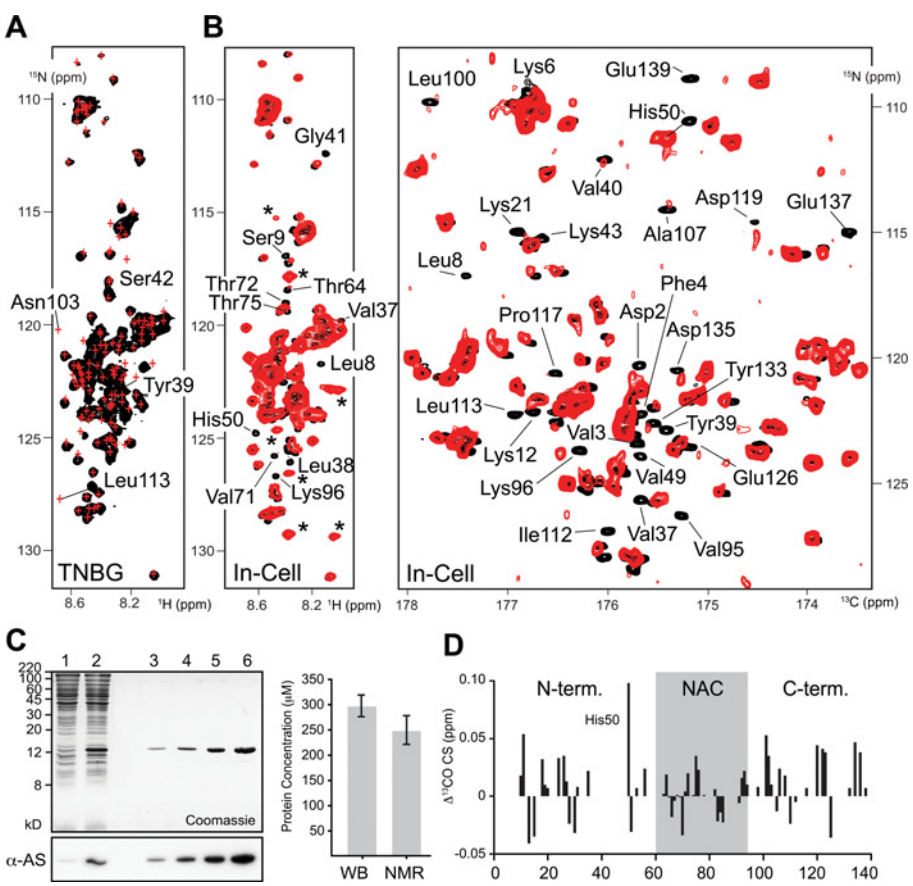

slurry. Two-dimensional in-cell NMR spectra then provide atomic-resolution details about the structural features of the overexpressed intracellular protein. A number of in-cell NMR studies of α-synuclein inside *E. coli* cells have been reported [21,43–48]. In all of these studies, in-cell NMR spectra of α-synuclein (^{1}H-^{15}N and ^{13}CO-^{15}N) and *in vitro* reference correlations of the protein purified under denaturing conditions looked remarkably similar. Our own in-cell NMR data corroborate this notion (Figure 1B). We, and others, interpret these findings as an indication for the preservation of the monomeric disordered protein state inside the crowded cytoplasm of live bacteria. Proponents of the tetramer hypothesis argue that these and other *E. coli* in-cell NMR spectra resemble cross-peak patterns of the folded tetramer, which they interpret as pointing towards a native oligomeric α-synuclein state inside bacterial cells [28].

To correlate the intracellular protein concentration of overexpressed α-synuclein in our in-cell NMR samples to the experimentally obtained NMR signal intensities, we employed quantitative Western blotting and two-dimensional NMR signal integration (Figures 1B and 1C). These measurements established that intracellular α-synuclein was present at a concentration of ∼300 μM, which corresponded well to the ∼250 μM of α-synuclein in-cell NMR signals that we recorded (see the Supplementary Online Data at http://www.biochemsoctrans.org/bst/040/bst0400950add.htm for details). This indicated that the majority of α-synuclein inside *E. coli* contributed to the NMR signals detected. If these in-cell NMR measurements were to report the presence of a folded tetramer, the overall NMR signal quality would be greatly impaired by the much lower tumbling rate in this high-viscosity environment [44]. Pielak and co-workers recently presented an elegant demonstration of this concept by recording in-cell NMR spectra of α-synuclein (14 kDa) covalently fused to ubiquitin (5 kDa) [47]. Only NMR signals of the disordered α-synuclein portion of this construct could be detected and these superimposed well on to reference cross-peaks of the disordered monomer. A similar scenario would be expected for the postulated tetramer for which the first 100 residues were speculated to form the α-helical core region, while the protein C-terminus remained more flexible [28]. No such NMR characteristics were observed in in-cell NMR experiments.

However, in-cell NMR spectra of α-synuclein did reveal regions of site-selective line broadening. These mapped to different portions of α-synuclein, interspersed throughout the primary amino acid sequence in a non-continuous fashion (Supplementary Figure S1B at http://www.biochemsoctrans.org/bst/040/bst0400950add.htm). In macromolecular crowded *in vitro* solutions (305 mg/ml BSA), α-synuclein displayed similar patterns of line broadening (Supplementary Figure S1A), which indicated that unspecific interactions with BSA (*in vitro*), or with cellular components in *E. coli* (in-cell) and/or conformational/chemical exchange effects could be causing this behaviour. To rule out chemical exchange contributions, we resorted to two-dimensional heteronuclear (^{13}CO-^{15}N) in-cell experiments, which do not involve exchangeable protons [49]. Direct carbon-detected ^{13}CO-^{15}N experiments have previously been employed to characterize bacterial in-cell α-synuclein samples [48]. Because ^{13}CO-^{15}N spectra display greater overall chemical shift dispersion, their use for residue-resolved analyses is advantageous over ^{1}H-^{15}N correlations. In addition, ^{13}C chemical shifts of backbone carbonyls are highly sensitive to changes in protein backbone conformations and are widely used as unbiased indicators for protein secondary structure [50,51]. Similar to the previous in-cell NMR study employing ^{13}CO-^{15}N experiments, our *in vivo* NMR data revealed α-synuclein ^{13}CO-^{15}N cross-peaks that closely matched the *in vitro* reference pattern of the disordered monomer (Figure 1B, right-hand panel). Minor chemical shift differences ($\delta\Delta_{CO}$ <0.07 p.p.m., with the exception of His^{50} which reported a slightly more basic intracellular pH) were detected throughout the protein (Figure 1D). Overall, no alterations in secondary structure were detected. Matching regions of site-selective line broadening were preserved under BSA-crowded *in vitro* conditions, although to a lesser extent (Supplementary Figure S1B). Moreover, when we lysed the in-cell NMR samples and recorded NMR spectra of the resulting extracts, the majority of the broadened NMR signals were recovered at nearly identical peak positions compared with *in vitro* reference spectra (Supplementary Figures S2C–S2D at http://www.biochemsoctrans.org/bst/040/bst0400950add.htm). Cell lysis was performed using a mild protocol [36] and without boiling or denaturing the extract. According to quantitative NMR peak volume analyses, the amount of α-synuclein that was present in this extract (∼260 μM) was comparable with the amount detected by in-cell NMR measurements. Together, this indicated that α-synuclein exhibited a disordered monomeric conformation inside live *E. coli* cells.

Conclusions

We have presented *in vitro* and in-cell NMR evidence that call into question the postulated tetramer conformation of α-synuclein. Although, strictly speaking, we cannot rule out other intracellular α-synuclein conformations, especially in higher eukaryotic cells, in-cell NMR data in *E. coli* strongly support the idea that at least in this cellular environment α-synuclein displays structural and dynamic properties of an intrinsically disordered monomer.

Acknowledgements

We thank Dr Linda Ball for carefully reading the paper and helpful comments, Dr Stamatios Liokatis and Dr Honor M. Rose for stimulating discussions, and Dr Peter Schmieder and Monika Beerbaum for NMR infrastructure support.

Funding

P.S. is a recipient of an Emmy Noether Programme grant [grant number SE-1794/1-1] by the Deutsche Forschungsgemeinschaft (DFG).

References

1 Goedert, M. (2001) α-Synuclein and neurodegenerative diseases. Nat. Rev. Neurosci. **2**, 492–501
2 Spillantini, M.G., Schmidt, M.L., Lee, V.M., Trojanowski, J.Q., Jakes, R. and Goedert, M. (1997) α-Synuclein in Lewy bodies. Nature **388**, 839–840
3 Bussell, Jr, R. and Eliezer, D. (2003) A structural and functional role for 11-mer repeats in α-synuclein and other exchangeable lipid binding proteins. J. Mol. Biol. **329**, 763–778
4 Jao, C.C., Der-Sarkissian, A., Chen, J. and Langen, R. (2004) Structure of membrane-bound α-synuclein studied by site-directed spin labeling. Proc. Natl. Acad. Sci. U.S.A. **101**, 8331–8336
5 Giasson, B.I., Murray, I.V., Trojanowski, J.Q. and Lee, V.M. (2001) A hydrophobic stretch of 12 amino acid residues in the middle of α-synuclein is essential for filament assembly. J. Biol. Chem. **276**, 2380–2386

6 Bertoncini, C.W., Jung, Y.S., Fernandez, C.O., Hoyer, W., Griesinger, C., Jovin, T.M. and Zweckstetter, M. (2005) Release of long-range tertiary interactions potentiates aggregation of natively unstructured α-synuclein. Proc. Natl. Acad. Sci. U.S.A. **102**, 1430–1435
7 Fernandez, C.O., Hoyer, W., Zweckstetter, M., Jares-Erijman, E.A., Subramaniam, V., Griesinger, C. and Jovin, T.M. (2004) NMR of α-synuclein-polyamine complexes elucidates the mechanism and kinetics of induced aggregation. EMBO J. **23**, 2039–2046
8 Hoyer, W., Cherny, D., Subramaniam, V. and Jovin, T.M. (2004) Impact of the acidic C-terminal region comprising amino acids 109–140 on α-synuclein aggregation *in vitro*. Biochemistry **43**, 16233–16242
9 Weinreb, P.H., Zhen, W., Poon, A.W., Conway, K.A. and Lansbury, Jr, P.T. (1996) NACP, a protein implicated in Alzheimer's disease and learning, is natively unfolded. Biochemistry **35**, 13709–13715
10 Uversky, V.N., Li, J. and Fink, A.L. (2001) Evidence for a partially folded intermediate in α-synuclein fibril formation. J. Biol. Chem. **276**, 10737–10744
11 Uversky, V.N., Li, J. and Fink, A.L. (2001) Metal-triggered structural transformations, aggregation, and fibrillation of human α-synuclein: a possible molecular link between Parkinson's disease and heavy metal exposure. J. Biol. Chem. **276**, 44284–44296
12 Hoyer, W., Antony, T., Cherny, D., Heim, G., Jovin, T.M. and Subramaniam, V. (2002) Dependence of α-synuclein aggregate morphology on solution conditions. J. Mol. Biol. **322**, 383–393
13 Uversky, V.N. (2003) A protein-chameleon: conformational plasticity of α-synuclein, a disordered protein involved in neurodegenerative disorders. J. Biomol. Struct. Dyn. **21**, 211–234
14 Uversky, V.N. and Fink, A.L. (2004) Conformational constraints for amyloid fibrillation: the importance of being unfolded. Biochim. Biophys. Acta **1698**, 131–153
15 Fink, A.L. (2006) The aggregation and fibrillation of α-synuclein. Acc. Chem. Res. **39**, 628–634
16 Binolfi, A., Rasia, R.M., Bertoncini, C.W., Ceolin, M., Zweckstetter, M., Griesinger, C., Jovin, T.M. and Fernandez, C.O. (2006) Interaction of α-synuclein with divalent metal ions reveals key differences: a link between structure, binding specificity and fibrillation enhancement. J. Am. Chem. Soc. **128**, 9893–9901
17 Bertoncini, C.W., Rasia, R.M., Lamberto, G.R., Binolfi, A., Zweckstetter, M., Griesinger, C. and Fernandez, C.O. (2007) Structural characterization of the intrinsically unfolded protein β-synuclein, a natural negative regulator of α-synuclein aggregation. J. Mol. Biol. **372**, 708–722
18 Paleologou, K.E., Schmid, A.W., Rospigliosi, C.C., Kim, H.Y., Lamberto, G.R., Fredenburg, R.A., Lansbury, Jr, P.T., Fernandez, C.O., Eliezer, D., Zweckstetter, M. and Lashuel, H.A. (2008) Phosphorylation at Ser-129 but not the phosphomimics S129E/D inhibits the fibrillation of α-synuclein. J. Biol. Chem. **283**, 16895–16905
19 Lamberto, G.R., Binolfi, A., Orcellet, M.L., Bertoncini, C.W., Zweckstetter, M., Griesinger, C. and Fernandez, C.O. (2009) Structural and mechanistic basis behind the inhibitory interaction of PcTS on α-synuclein amyloid fibril formation. Proc. Natl. Acad. Sci. U.S.A. **106**, 21057–21062
20 Bussell, Jr, R. and Eliezer, D. (2001) Residual structure and dynamics in Parkinson's disease-associated mutants of α-synuclein. J. Biol. Chem. **276**, 45996–46003
21 Croke, R.L., Sallum, C.O., Watson, E., Watt, E.D. and Alexandrescu, A.T. (2008) Hydrogen exchange of monomeric α-synuclein shows unfolded structure persists at physiological temperature and is independent of molecular crowding in *Escherichia coli*. Protein Sci. **17**, 1434–1445
22 Dedmon, M.M., Lindorff-Larsen, K., Christodoulou, J., Vendruscolo, M. and Dobson, C.M. (2005) Mapping long-range interactions in α-synuclein using spin-label NMR and ensemble molecular dynamics simulations. J. Am. Chem. Soc. **127**, 476–477
23 Lee, J.C., Gray, H.B. and Winkler, J.R. (2005) Tertiary contact formation in α-synuclein probed by electron transfer. J. Am. Chem. Soc. **127**, 16388–16389
24 Lee, J.C., Lai, B.T., Kozak, J.J., Gray, H.B. and Winkler, J.R. (2007) α-Synuclein tertiary contact dynamics. J. Phys. Chem. B **111**, 2107–2112
25 Jensen, M.R., Communie, G., Ribeiro, Jr, E.A., Martinez, N., Desfosses, A., Salmon, L., Mollica, L., Gabel, F., Jamin, M., Longhi, S. et al. (2011) Intrinsic disorder in measles virus nucleocapsids. Proc. Natl. Acad. Sci. U.S.A. **108**, 9839–9844
26 Wells, M., Tidow, H., Rutherford, T.J., Markwick, P., Jensen, M.R., Mylonas, E., Svergun, D.I., Blackledge, M. and Fersht, A.R. (2008) Structure of tumor suppressor p53 and its intrinsically disordered N-terminal transactivation domain. Proc. Natl. Acad. Sci. U.S.A. **105**, 5762–5767
27 Bartels, T., Choi, J.G. and Selkoe, D.J. (2011) α-Synuclein occurs physiologically as a helically folded tetramer that resists aggregation. Nature **477**, 107–110
28 Wang, W., Perovic, I., Chittuluru, J., Kaganovich, A., Nguyen, L.T., Liao, J., Auclair, J.R., Johnson, D., Landeru, A., Simorellis, A.K. et al. (2011) A soluble α-synuclein construct forms a dynamic tetramer. Proc. Natl. Acad. Sci. U.S.A. **108**, 17797–17802
29 Bussell, Jr, R., Ramlall, T.F. and Eliezer, D. (2005) Helix periodicity, topology, and dynamics of membrane-associated α-synuclein. Protein Sci. **14**, 862–872
30 Ulmer, T.S., Bax, A., Cole, N.B. and Nussbaum, R.L. (2005) Structure and dynamics of micelle-bound human α-synuclein. J. Biol. Chem. **280**, 9595–9603
31 Eliezer, D., Kutluay, E., Bussell, Jr, R. and Browne, G. (2001) Conformational properties of α-synuclein in its free and lipid-associated states. J. Mol. Biol. **307**, 1061–1073
32 Sung, Y.H. and Eliezer, D. (2007) Residual structure, backbone dynamics, and interactions within the synuclein family. J. Mol. Biol. **372**, 689–707
33 Alves, V.S. and Castilho, B.A. (2005) Gir2 is an intrinsically unstructured protein that is present in *Saccharomyces cerevisiae* as a group of heterogeneously electrophoretic migrating forms. Biochem. Biophys. Res. Commun. **332**, 450–455
34 Kaplon, T.M., Michnik, A., Drzazga, Z., Richter, K., Kochman, M. and Ozyhar, A. (2009) The rod-shaped conformation of Starmaker. Biochim. Biophys. Acta **1794**, 1616–1624
35 Zeev-Ben-Mordehai, T., Rydberg, E.H., Solomon, A., Toker, L., Auld, V.J., Silman, I., Botti, S. and Sussman, J.L. (2003) The intracellular domain of the *Drosophila* cholinesterase-like neural adhesion protein, gliotactin, is natively unfolded. Proteins **53**, 758–767
36 Fauvet, B., Mbefo, M.K., Fares, M.B., Desobry, C., Michael, S., Ardah, M.T., Tsika, E., Coune, P., Prudent, M., Lion, N. et al. (2012) α-Synuclein in central nervous system and from erythrocytes, mammalian cells, and *Escherichia coli* exists predominantly as a disordered monomer. J. Biol. Chem. **287**, 15345–15364
37 Trexler, A.J. and Rhoades, E. (2012) N-terminal acetylation is critical for forming α-helical oligomer of α-synuclein. Protein Sci. **21**, 601–605
38 Ito, Y. and Selenko, P. (2010) Cellular structural biology. Curr. Opin. Struct. Biol. **20**, 640–648
39 Selenko, P. and Wagner, G. (2007) Looking into live cells with in-cell NMR spectroscopy. J. Struct. Biol. **158**, 244–253
40 Serber, Z., Corsini, L., Durst, F. and Dotsch, V. (2005) In-cell NMR spectroscopy. Methods Enzymol. **394**, 17–41
41 Serber, Z., Ledwidge, R., Miller, S.M. and Dotsch, V. (2001) Evaluation of parameters critical to observing proteins inside living *Escherichia coli* by in-cell NMR spectroscopy. J. Am. Chem. Soc. **123**, 8895–8901
42 Robinson, K.E., Reardon, P.N. and Spicer, L.D. (2012) In-cell NMR spectroscopy in *Escherichia coli*. Methods Mol. Biol. **831**, 261–277
43 Barnes, C.O. and Pielak, G.J. (2011) In-cell protein NMR and protein leakage. Proteins **79**, 347–351
44 Li, C., Charlton, L.M., Lakkavaram, A., Seagle, C., Wang, G., Young, G.B., Macdonald, J.M. and Pielak, G.J. (2008) Differential dynamical effects of macromolecular crowding on an intrinsically disordered protein and a globular protein: implications for in-cell NMR spectroscopy. J. Am. Chem. Soc. **130**, 6310–6311
45 McNulty, B.C., Young, G.B. and Pielak, G.J. (2006) Macromolecular crowding in the *Escherichia coli* periplasm maintains α-synuclein disorder. J. Mol. Biol. **355**, 893–897
46 Sharaf, N.G., Barnes, C.O., Charlton, L.M., Young, G.B. and Pielak, G.J. (2010) A bioreactor for in-cell protein NMR. J. Magn. Reson. **202**, 140–146
47 Barnes, C.O., Monteith, W.B. and Pielak, G.J. (2011) Internal and global protein motion assessed with a fusion construct and in-cell NMR spectroscopy. ChemBioChem **12**, 390–391
48 Bertini, I., Felli, I.C., Gonnelli, L., Kumar, M.V.V. and Pierattelli, R. (2011) ^{13}C direct-detection biomolecular NMR spectroscopy in living cells. Angew. Chem. Int. Ed. **50**, 2339–2341
49 Bermel, W., Bertini, I., Felli, I.C. and Pieratelli, R. (2009) Speeding up ^{13}C direct detection biomolecular NMR spectroscopy. J. Am. Chem. Soc. **131**, 15339–15345
50 Wishart, D.S. and Sykes, B.D. (1994) The ^{13}C chemical-shift index: a simple method for the identification of protein secondary structure using ^{13}C chemical-shift data. J. Biomol. NMR **4**, 171–180
51 Wishart, D.S. and Sykes, B.D. (1994) Chemical shifts as a tool for structure determination. Methods Enzymol. **239**, 363–392

Received 11 April 2012
doi:10.1042/BST20120096

SUPPLEMENTARY ONLINE DATA

Bacterial in-cell NMR of human α-synuclein: a disordered monomer by nature?

Andres Binolfi, Francois-Xavier Theillet and Philipp Selenko[1]

In-cell NMR Group, Department of NMR-Assisted Structural Biology, Leibniz Institute of Molecular Pharmacology (FMP Berlin), Robert-Roessle-Strasse 10, Berlin 13125, Germany

Materials and methods

Proteins and reagents

^{15}N and ^{15}N/^{13}C isotope-labelled α-synuclein for *in vitro* NMR experiments was obtained by overexpression of a pT-T7 plasmid containing full-length α-synuclein in *E. coli* BL21(DE3) cells using M9 minimal medium supplemented with $^{15}NH_4Cl$ and [^{13}C]glucose (Sigma). Purification of the disordered monomer included a boiling step to initially clear the bacterial lysate after expression of recombinant α-synuclein, as reported previously [1]. Protein samples were dissolved in 20 mM phosphate buffer supplemented with 150 mM NaCl at pH 7.0 (NMR buffer). BSA was purchased from Carl Roth.

In-cell NMR samples

In-cell NMR samples were generated following the protocol by Robinson et al. [2]. In brief, a 20 ml α-synuclein overnight LB (Luria–Bertani) culture of transformed *E. coli* cells was used to inoculate a 400 ml LB culture (non-isotope-labelled). After reaching a D_{600} of ~0.8, cells were harvested by centrifugation at 3000 ***g*** for 10 min. The cell pellet was washed once with M9 minimal medium to remove any remaining LB. Washed cells were inoculated in 100 ml of M9 minimal medium and induced with 1 mM IPTG (isopropyl β-D-thiogalactopyranoside) for 4 h at 37°C. Cells were gently harvested and washed twice with NMR buffer. The final cell pellet (~600 μl) was resuspended with 200 μl of NMR buffer supplemented with 10% ^2H_2O and the cell slurry was loaded into a 5 mm NMR tube. Lysis of the *E. coli* cell slurry after in-cell NMR measurements was performed by sonication on ice using a digital sonifier (Branson) and according to the bacterial lysis protocol described by Fauvet et al. [3]. The lysate/extract was cleared by centrifugation at 17000 ***g*** for 25 min at 4°C. NMR spectra were acquired directly on the cleared lysate/extract.

NMR acquisition, data processing and analysis

All NMR spectra were recorded in 5 mm NMR tubes on a 750 MHz Bruker Avance spectrometer, equipped with a cryogenically cooled triple resonance ^{1}H{^{13}C/^{15}N} TCI probe. In-cell ^{1}H-^{15}N correlations were obtained using two-dimensional ^{1}H-^{15}N SOFAST-HMQC (band-selective optimized flip-angle short-transient heteronuclear multiple quantum coherence) experiments [4] at 10°C. NMR spectra were acquired with 1024 and 256 complex points in the ^{1}H and ^{15}N dimensions respectively and 32 scans. Pulses, delays and decoupling schemes have been reported previously [5]. *In vitro* reference NMR spectra of the disordered monomer were recorded on 50–250 μM α-synuclein samples dissolved in NMR buffer. Unless otherwise specified, all NMR spectra were collected on samples dissolved in buffer at pH 7.0. All SOFAST-HMQC NMR spectra were zero-filled to 4096 and 2048 points for the ^{1}H and ^{15}N dimensions respectively. Equal numbers of real points in the ^{15}N dimension were linear-predicted for in-cell and *in vitro* samples. In-cell (H-flip)^{13}CO-^{15}N experiments [6] were recorded at 30°C. ^{13}CO-^{15}N spectra were acquired with 1024 complex points for the ^{13}CO dimension and 64 increments for the ^{15}N dimension [resulting from 128 IPAP (in-phase/antiphase) increments] with 256 scans. Pulses, delays and decoupling schemes have been reported previously [5]. *In vitro* reference NMR spectra of the disordered monomer were recorded on 250 μM α-synuclein samples dissolved in NMR buffer. NMR parameters for *in vitro* α-synuclein samples were 1024 complex points in the ^{13}CO dimension and 128 increments in the ^{15}N dimension (resulting from 256 IPAP increments) with 256 scans. All ^{13}CO-^{15}N NMR spectra were zero-filled to 4096 and 2048 for the ^{1}H and ^{15}N dimensions respectively. Equal numbers of real points in the ^{15}N dimension were linear-predicted for in-cell and *in vitro* samples. *In vitro* crowding NMR spectra were recorded in NMR buffer at pH 6.4 supplemented with 305 mg/ml BSA and identical spectrometer settings. All NMR spectra were processed with Topspin 2.3 (Bruker) and analysed using Topspin and Sparky 3 (http://www.cgl.ucsf.edu/home/sparky/).

SDS/PAGE, Western blotting and protein quantification

A 25 μl volume of the *E. coli* cell suspension was removed before and after IPTG induction, diluted into a 225 μl

[1]To whom correspondence should be addressed (email selenko@fmp-berlin.de).

final volume of SDS sample buffer supplemented with 2-mercaptoethanol and boiled for 5 min. Aliquots of 4 μl were diluted further into a final volume of 20 μl, of which two 10 μl amounts were loaded on to two denaturing SDS 18% polyacrylamide gels. The final dilution factor was 45. A dilution series of reference α-synuclein concentrations were loaded on to both gels for Western blot quantifications. Reference concentrations were 3.5, 7.0, 14 and 28 μM α-synuclein. SDS/PAGE was performed on Miniprotean III systems (Bio-Rad Laboratories) in Tris/glycine buffer. One gel was stained with Coomassie Brilliant Blue, and the other was transferred on to nitrocellulose for Western blotting (Turbo transfer system, Bio-Rad Laboratories). Molecular-mass markers for SDS/PAGE were Color-Burst markers (Sigma). Western blot membranes were blocked with 5% (w/v) non-fat dried milk powder dissolved in TBS (100 mM Tris/HCl, pH 7.5, and 0.9% NaCl) for 1 h at room temperature. Membranes were incubated with primary antibody overnight at 4°C: monoclonal anti-(N-terminal α-synuclein) (Abcam ab51252, 1:500 dilution in TBS supplemented with 0.1% Tween 20). Membranes were processed using standard protocols and incubated with HRP (horseradish peroxidase)-conjugated secondary antibody (Sigma A6667, anti-rabbit, dilution 1:10 000 in TBS supplemented with 0.1% Tween 20). HRP chemiluminescence was probed with 1 ml of Super Signal West Pico (ThermoScientific). Exposures of 2 min were visualized using the ChemiDoc XRS Imaging System (Bio-Rad Laboratories).

Quantification of protein concentrations

Protein concentrations were determined by quantitative Western blotting and NMR signal integration. In brief, Western blot band intensities of α-synuclein references were quantified using the ImageLab software package (Bio-Rad Laboratories) by obtaining calibration curves to which in-cell concentrations of α-synuclein were correlated. Quantifications of two-dimensional NMR signals were performed by integrating selected sets of well-resolved NMR cross-peaks from in-cell ^{1}H-^{15}N SOFAST-HMQC NMR spectra and by comparing the signal intensities obtained with *in vitro* reference samples of the disordered monomer at known concentrations. The integration tool in Topspin 2.3 was used for quantifying peak volumes. Only non-overlapped NMR cross-peaks were taken into account, i.e. Gly^{31}, Gly^{67}, Gly^{68}, Gly^{73}, Gly^{86}, Gly^{93}, Thr^{92}, Asn^{103}, Asp^{119}, Ser^{129} and Ala^{140} for both in-cell and NMR lysate samples.

Figure S1 | **Comparison of α-synuclein NMR properties inside *E. coli* cells and in 305 mg/ml BSA**

(**A**) Schematic representation of the broadening profile observed in both environments for two-dimensional ^{1}H-^{15}N SOFAST-HMQC (upper panel) and (H-flip)^{13}CO-^{15}N (lower panel) experiments/NMR spectra. Broadened α-synuclein residues unambiguously identified in different protein regions are shown as grey boxes. Red lines represent NMR signal intensity ratios (I/I_{ref}) for α-synuclein in BSA (over *in vitro*) obtained from two-dimensional ^{1}H-^{15}N and ^{13}CO-^{15}N correlation experiments. Only well-resolved isolated NMR peaks were used for the analysis. (**B**) Overlay of two-dimensional ^{1}H-^{15}N SOFAST-HMQC (left) and two-dimensional (H-flip)^{13}CO-^{15}N (right) NMR spectra of α-synuclein *in vitro* (black) and in the presence of 305 mg/ml BSA (red). NMR spectra were recorded on 200 μM α-synuclein samples dissolved in NMR buffer at pH 6.4 and 15°C to minimize solvent-exchange effect contributions (i.e. line-broadening).

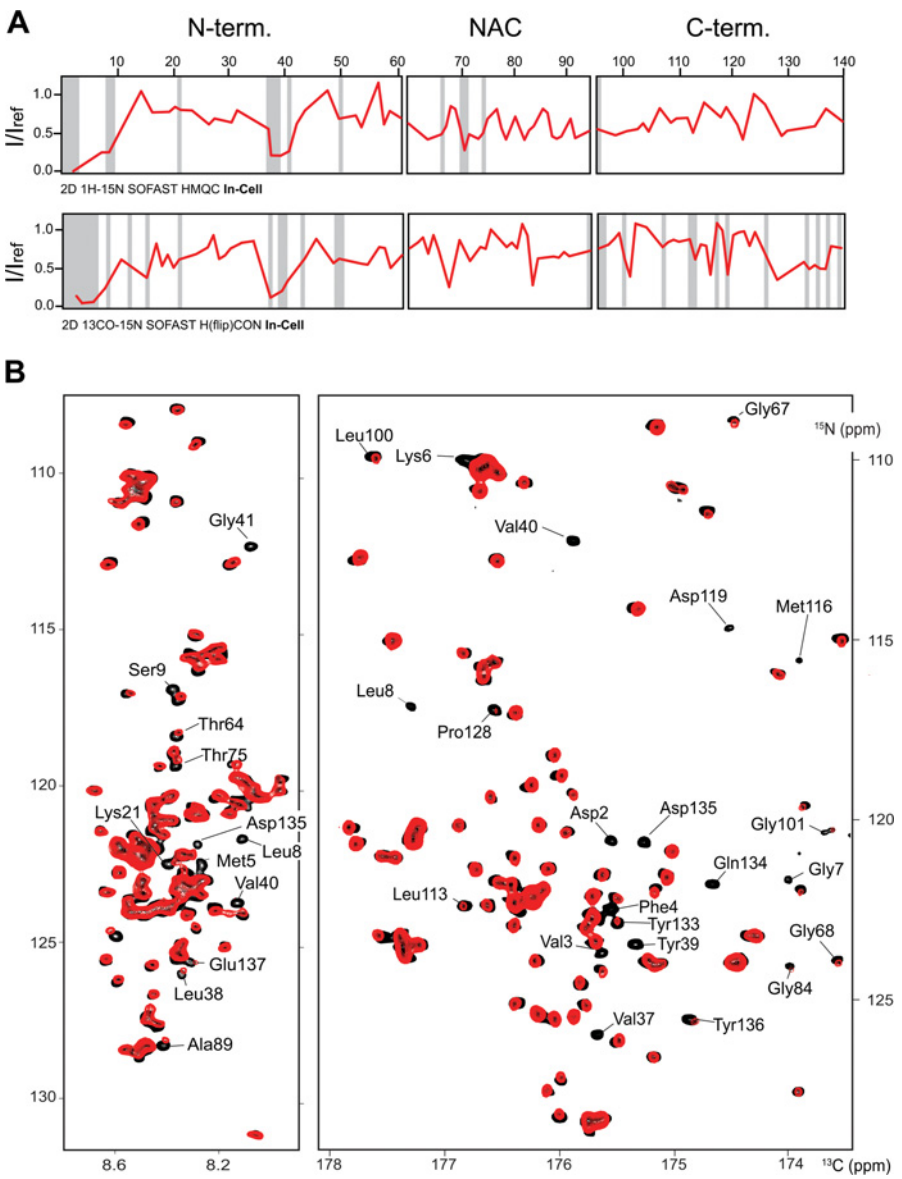

Figure S2 | In-cell NMR control experiments

(**A**) Overlay of two-dimensional ^{1}H-^{15}N SOFAST HMQC spectra of monomeric α-synuclein *in vitro* (black) and of non-transformed *E. coli* cells grown in isotope-labelled ($^{15}NH_4Cl$ and/or [^{13}C]glucose) M9 minimal medium, induced for 4 h (red). NMR resonances of isotope-labelled background metabolites are clearly visible. These are also present in the in-cell NMR spectrum of overexpressed α-synuclein in Figure 1(B) of the main text (some marked with an asterisk). (**B**) Overlay of two-dimensional ^{1}H-^{15}N SOFAST-HMQC spectra of monomeric α-synuclein *in vitro* (black) and of the *E. coli* supernatant recovered after in-cell NMR measurements by gentle sedimentation of the cell slurry. Only minor α-synuclein NMR signals (<1%) were detected, indicating that no significant protein leakage had occurred during the in-cell NMR experiment. Contour levels are the same as in Figure 1(B) of the main text. (**C**) Two-dimensional overlay of ^{1}H-^{15}N SOFAST-HMQC and (**D**) two-dimensional (H-flip)^{13}CO-^{15}N spectra of monomeric α-synuclein *in vitro* (black) and the in-cell NMR sample after cell lysis (red). Chemical shift differences of α-synuclein residues close to His^{50} can be attributed to small changes in pH between *in vitro* and cell lysate solutions. We are currently investigating the causes for the chemical shift/line-broadening effects of Glu^{57}, Val^{66}, Lys^{80}, Pro^{117} and Glu^{139} in the lysate ^{13}CO-^{15}N spectrum.

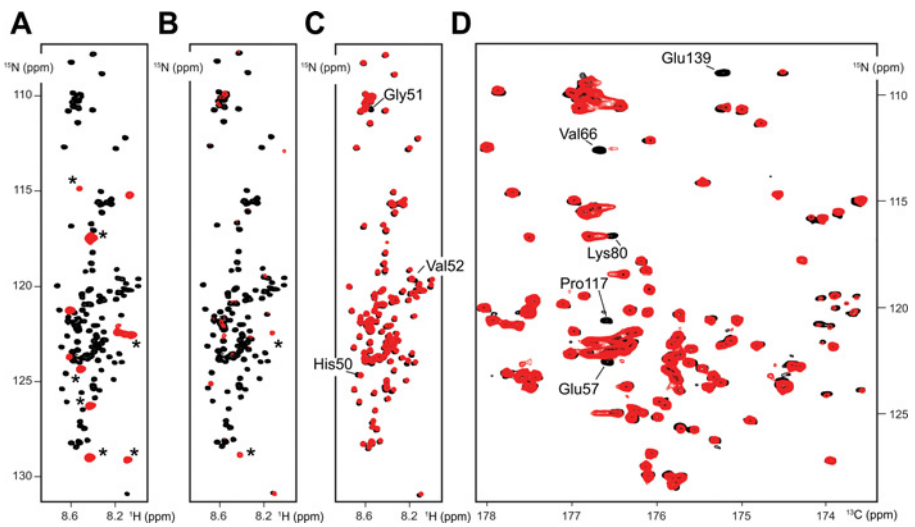

References

1 Hoyer, W., Antony, T., Cherny, D., Heim, G., Jovin, T.M. and Subramaniam, V. (2002) Dependence of α-synuclein aggregate morphology on solution conditions. J. Mol. Biol. **322**, 383–393

2 Robinson, K.E., Reardon, P.N. and Spicer, L.D. (2012) In-cell NMR spectroscopy in *Escherichia coli*. Methods Mol. Biol. **831**, 261–277

3 Fauvet, B., Mbefo, M.K., Fares, M.B., Desobry, C., Michael, S., Ardah, M.T., Tsika, E., Coune, P., Prudent, M., Lion, N. et al. (2012) α-Synuclein in central nervous system and from erythrocytes, mammalian cells, and *Escherichia coli* exists predominantly as a disordered monomer. J. Biol. Chem. **287**, 15345–15364

4 Schanda, P., Kupce, E. and Brutscher, B. (2005) SOFAST-HMQC experiments for recording two-dimensional heteronuclear correlation spectra of proteins within a few seconds. J. Biomol. NMR **33**, 199–211

5 Theillet, F.X., Binolfi, A., Liokatis, S., Verzini, S. and Selenko, P. (2011) Paramagnetic relaxation enhancement to improve sensitivity of fast NMR methods: applications to intrinsically disordered proteins. J. Biomol. NMR **51**, 487–495

6 Bermel, W., Bertini, I., Felli, I.C. and Pieratelli, R. (2009) Speeding up ^{13}C direct detection biomolecular NMR spectroscopy. J. Am. Chem. Soc. **131**, 15339–15345

Received 11 April 2012
doi:10.1042/BST20120096